Theory & Computation

Rate coefficients in a degenerate plasma produced by short wavelength lasers

V. Aslanyan, G. J. Tallents *(York Plasma Institute, University of York, UK)*

We have constructed a collisional-radiative model, with rate coefficients calculated using the Fermi-Dirac energy distribution function for free electrons. This allowed us to compare how the steady-state and time-evolved ionization fraction in plasmas vary from calculations, assuming the usual Maxwell-Boltzmann electron distribution, for different laser intensities.

We have found that, although the Fermi-Dirac distribution makes little difference for plasma conditions close to local thermodynamic equilibrium, the presence of strong photoionizing radiation, such as that from a short wavelength laser, creates dense and degenerate electrons. The evolution of a degenerate plasma may differ significantly from a classical plasma.

Contact: V. Aslanyan (va567@york.ac.uk)

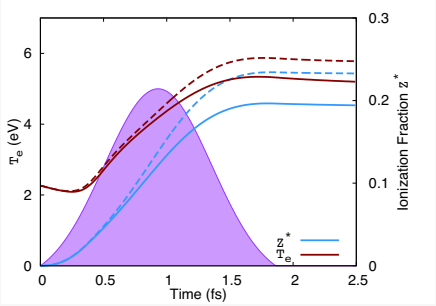

Ionization fraction and temperature evolution of diamond as it is subjected to a pulse of short wavelength radiation (photon energy – 14 eV, duration – 1 fs, peak intensity – 10^{14} W cm^{-2}). The dashed lines assume a Maxwell-Boltzmann electron distribution, while the solid lines assume a Fermi-Dirac distribution.

Shrinking the angular distribution of fast electrons via wires with an inverse conical taper

A.P.L. Robinson, H. Schmitz *(Plasma Physics Group, CLF, STFC Rutherford Appleton Laboratory, Didcot, UK)*

We report on our recent studies of targets that exploit resistivity gradients to guide fast electrons and which incorporate an inverse conical taper. This is perhaps the simplest geometry that is interesting in terms of its ability to reduce the angular spread of the fast electrons. We also show how this can be applied to wire heating and the remarkable improvement that including even a slight inverse conical taper can yield.

Contact: A. Robinson (alex.robinson@stfc.ac.uk)

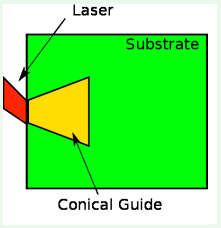

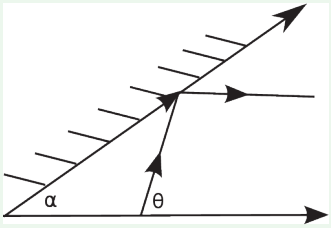

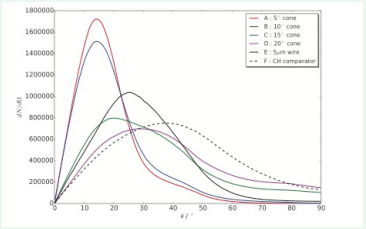

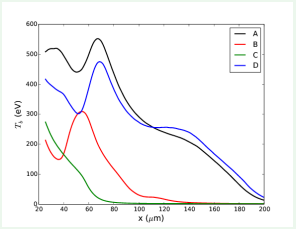

Top left: Schematic plot of wire with inverse conical taper.
Top right: Schematic plot of reflection from oblique plane.
Bottom left: Angular distribution of fast electrons from different simulations. Legend indicates type of guide element used in each simulation. Distributions are calculated at 3 ps (substantially after end of injection).
Bottom right: Lineouts (along guide axis) of background electron temperature (eV) in simulations with different wire targets, with/without inverse conical tapers.

The effect of superluminal phase velocity on electron acceleration in a powerful electromagnetic wave

A.P.L. Robinson *(Plasma Physics Group, CLF, STFC Rutherford Appleton Laboratory, Didcot, UK)*
A.V. Arefiev, V.N. Khudik *(Institute for Fusion Studies, The University of Texas, USA)*

We have derived an analytic solution for the problem of a single electron in an electromagnetic (EM) plane wave of arbitrary strength and arbitrary phase velocity. The solution has been checked against direct numerical integration. From this analytic solution we can begin to understand the extent to which EM dispersion (and thus superluminal phase velocities), due to either plasma dispersion or wave-guiding, affects direct laser acceleration (DLA).

Contact: A. Robinson (alex.robinson@stfc.ac.uk)

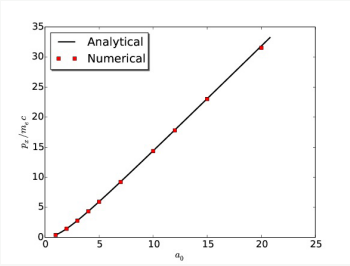

Top: Peak longitudinal momentum p_x from a series of numerical calculations in which a_0 is varied for v_p = 1.15c against the predictions of equation 16:

$$\frac{p_\parallel}{m_e c} = \tilde{p}_x = \frac{\sqrt{u^2 + a^2(u^2-1)} - u}{u^2 - 1}$$

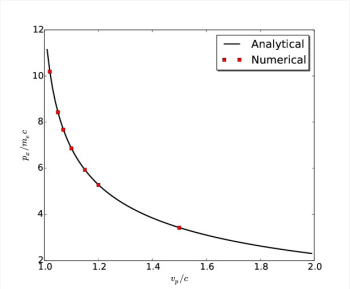

Bottom: Peak longitudinal momentum p_x from a series of numerical calculations in which v_p is varied for a_0 = 5 against the predictions of equation 16.

Anisotropic cooling of electron beams interacting with intense laser pulses

A. Noble, S.R. Yoffe, D.A. Jaroszynski *(SUPA/Dept of Physics, University of Strathclyde, Glasgow, UK)*

With the advent of a new breed of high power laser facility, it is essential to understand the dynamics of relativistic electron beams interacting with ultra-intense laser pulses, such as the reduction of their momentum spread. We have explored a prime example of such effects, namely the radiative reduction of momentum spread, or beam cooling.

Ignoring radiation reaction, there is no beam cooling: electrons emerge from the pulse with their initial momentum spread. The situation is changed when radiation reaction is included. According to the classical theory, interaction with the pulse causes significant beam cooling, which is equally partitioned between transverse and longitudinal directions. Including quantum effects changes things once again, with a reduction in beam cooling, and a breaking of the symmetry between longitudinal and transverse directions, with the transverse cooling lying closer to the classical case, and the longitudinal cooling more resembling the case with no radiation reaction. In all cases there is isotropy within the transverse plane, the polarisation of the laser pulse playing no role.

Contact: A. Noble (adam.noble@strath.ac.uk)

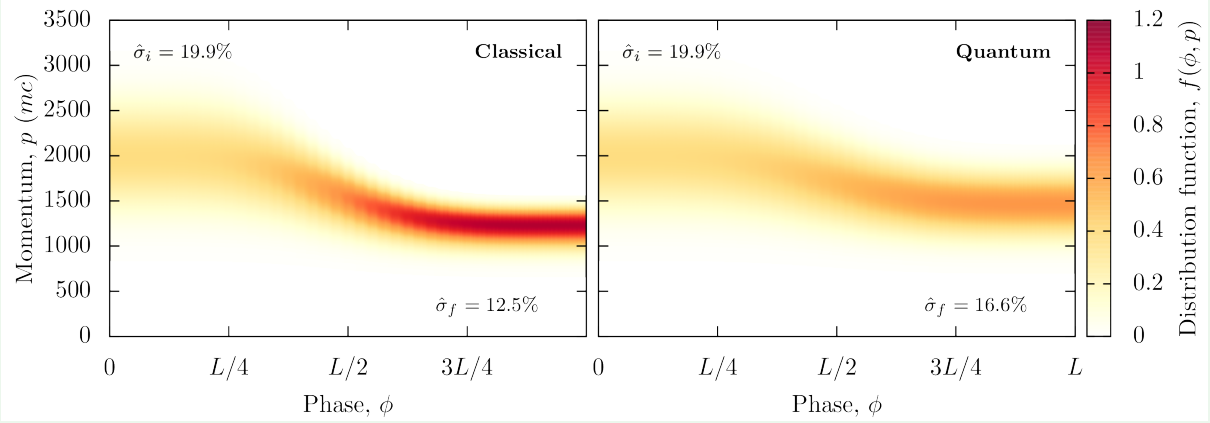

Longitudinal cooling of a 1 GeV electron beam colliding with a 2 x 10^{21} W/cm² laser pulse.

Weak collisionless shocks in laser plasmas

R.A. Cairns *(University of St Andrews, Fife, UK)*
R. Bingham *(University of Strathclyde, Glasgow, UK; CLF, STFC Rutherford Appleton Laboratory, Didcot, UK)*
R. Trines *(CLF, STFC Rutherford Appleton Laboratory, Didcot, UK)*
P. Norreys *(CLF, STFC Rutherford Appleton Laboratory, Didcot, UK; Dept of Physics, University of Oxford, Oxford, UK)*

Last year we described a theory of low Mach number laminar collisionless shocks, and their possible relevance to observed localized high electric fields in laser compressed pellets and experiments on ion acceleration. Here we have extended our earlier work to look at more general properties of these structures, in order to obtain the parameter domain within which they exist and some scaling laws. In a single species plasma, there are two parameters that determine the structure: the ratio of electron to ion temperature, and the Mach number.

The accompanying figures shows the domain of existence of the structures, with a minimum temperature ratio of just under 15 and a widening range of Mach numbers above this value. Within this range, a fairly small fraction of the ions is reflected, while above the maximum Mach number we expect a more complicated structure, with a large fraction of the ions reflected.

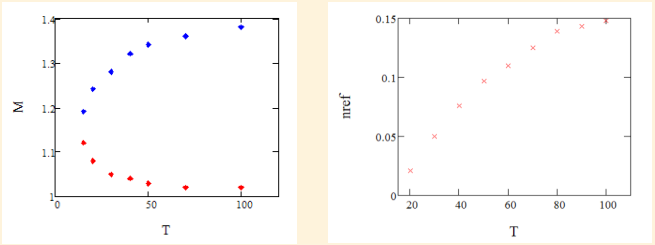

Left: Upper (blue) and lower (red) limits of the allowed Mach number range, estimated by numerical trial and error for a range of electron/ion temperature ratios.
Right: The reflected ion density as a function of temperature at the maximum Mach number.

Contact: R. A. Cairns (rac@st-andrews.ac.uk)

Single shot quantitative and spatially resolved plasma wakefield diagnostics

M.F. Kasim, J. Holloway, L. Ceurvorst, M. Levy, N. Ratan, J. Sadler, P.N. Burrows, P. Norreys *(Dept of Physics, University of Oxford, UK)*
R. Bingham, R. Trines *(CLF, STFC Rutherford Appleton Laboratory, Didcot, UK)*
M. Wing *(Dept of Physics & Astronomy, University College London, UK)*

Plasma wakefield accelerators are promising technology to accelerate particles within a distance up to three orders of magnitude shorter than conventional accelerators. However, only a few techniques exist to diagnose the plasma wakefields, and none of them can be used to quantitatively measure the amplitude of the wakefield in spatially-resolved manner. We propose a method to diagnose the plasma wakefield's parameters using photon acceleration. In this technique, a laser pulse that could cover several plasma wavelengths is fired into the wakefield. Inverting the measured frequency modulation profile of the pulse yields the density profile of the wakefield at the interaction point. By introducing a crossing angle the interaction point can be chosen, thus making it possible to diagnose the wakefield at certain positions in the plasma.

Simulations were performed to check the accuracy of the measured wakefield amplitude compared with the actual amplitude. Most of these results agree qualitatively and quantitatively, with a relative error less than 10% for various tested wakefield amplitudes, crossing angles and probe frequencies. This technique opens up new possibilities for qualitative and quantitative diagnostics of plasma wakefield density at chosen positions in a plasma.

Contact: M. F. Kasim (m.kasim1@physics.ox.ac.uk)

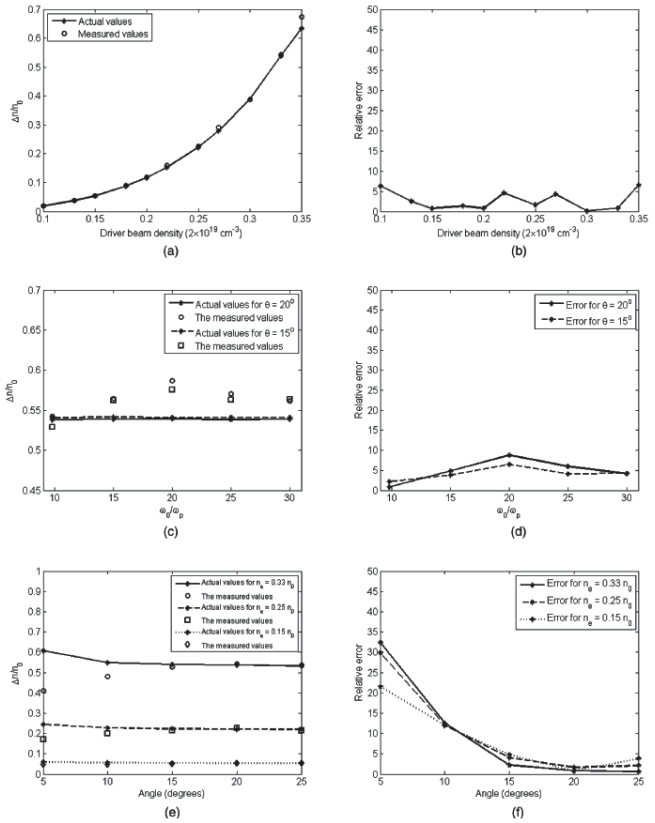

Comparison of the amplitude values between the measured and actual density profiles for (a) various peak driver beam density values and (b) the relative errors, (c) various probe frequencies and (d) its relative errors, and (e) various crossing angles with (f) its relative errors.

Measuring radiation reaction in laser-electron beam collisions

T. G. Blackburn
(Dept of Physics, Chalmers University of Technology, Gothenburg, Sweden)

Using today's high-power laser facilities, it is possible to detect quantum radiation reaction in the collision of a GeV electron beam and an intense laser pulse. Experimental signatures of radiation reaction will be the substantial yield of >10 MeV gamma rays and the reduced energy of the electron beam. This will still be evident even if that electron beam is accelerated by a laser wakefield, and so has a broad initial energy spectrum with a large low-energy tail.

We can exploit the fact that the diameter of the laser pulse will be smaller than that of the electron beam, and consider the latter's energy spectrum per unit cross-sectional area. As shown in the figure, there will be a prominent depletion zone in the areal energy spectrum if the beams collide successfully.

Contact: T. G. Blackburn (tom.blackburn@chalmers.se)

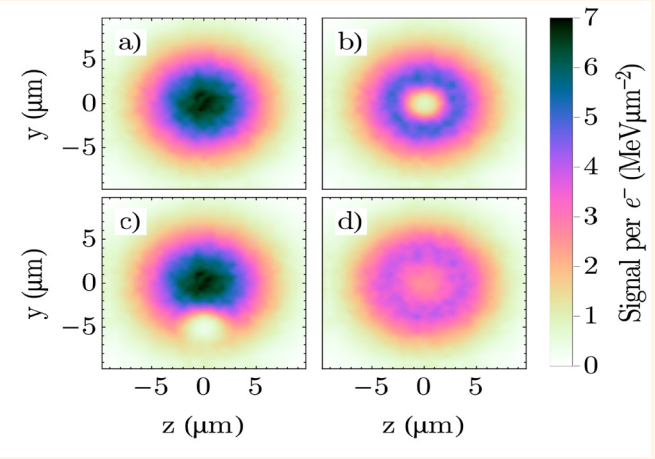

The energy carried by the electron beam, per particle per unit cross-sectional area a) prior to the collision with the high-intensity laser pulse, and immediately after a collision at b) Δx = Δy = 0, c) Δx = 0, Δy = 5 μm and d) Δx = 50 μm, Δy = 0.

Exploiting the self-similar nature of Raman and Brillouin scattering

R. M. G. M. Trines *(CLF, STFC Rutherford Appleton Laboratory, Didcot, UK)*

Raman and Brillouin amplification are two schemes for amplifying and compressing short laser pulses in plasma. Depending on the laser and plasma configurations, these schemes could potentially deliver the high-energy, high-power pulses needed for inertial confinement fusion, especially fast-ignition fusion.

Analytical self-similar models for both Raman and Brillouin amplification have already been derived [1,2], but the consequences of this self-similar behaviour are little known and hardly ever put to good use. In this paper, we will give an overview of the self-similar laws that govern the evolution of the probe pulse in Raman and Brillouin amplification. We will then show how these laws can be exploited, in particular regarding the parameters of the initial probe pulse, to control the properties of the final amplified probe and improve the efficiency of the process.

[1] V.M. Malkin, G. Shvets and N.J. Fisch, Phys. Rev. Lett. 82, 4448 (1999).
[2] A.A. Andreev et al., Phys. Plasmas 13, 053110 (2006).

Contact: R. Trines (raoul.trines@stfc.ac.uk)

Simulations of nanosecond laser self-focusing and channelling in under-dense magnetised plasmas

M. P. Read *(York Plasma Institute, University of York, UK; Imperial College London, UK)*
R. J. Kingham *(Blackett Laboratory Imperial College London, UK)*
P. A. Norreys *(Clarendon Laboratory, University of Oxford, UK; CLF, STFC Rutherford Appleton Laboratory, Didcot, UK)*

Magnetic fields – both applied and self-generated – are increasingly relevant to laser-plasma interactions, because of the potential benefits to ICF and plasma waveguide applications. Electron transport dynamics in magnetised plasmas are intricate, as heat-flow and B-field evolution feedback onto each other. To investigate laser self-focusing dynamics in such systems, two existing codes – CTC, a fluid code, and IMPACT, a VFP code – have been augmented with a paraxial wave solving module.

The fluid simulations of beam propagation through magnetised plasmas show significant changes in the electron density profile. These changes result in laser beam defocusing when Nernst advection is accounted for (see figure). Matching simulations using IMPACT, however, indicate that non-local effects are present and the fluid code can overestimate Nernst advection under these conditions. This highlights the need for appropriate heat flux and magnetic flux limitation.

Contact: M. P. Read (martin.read@york.ac.uk)

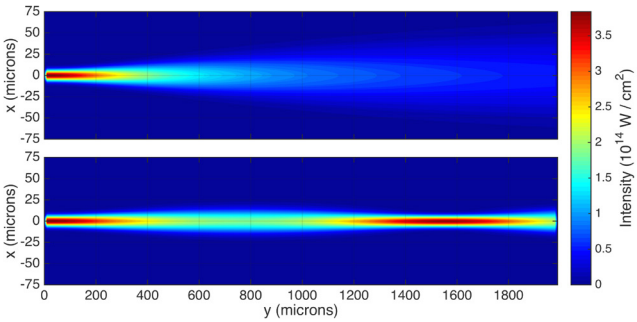

Laser intensity profiles from the fluid code CTC with Nernst advection enabled (upper) and disabled (lower). The laser defocuses after ~350 ps with Nernst advection accounted for,whereas without the beam is channelled over a distance of 2 mm.

The effect of lattice structure on fast electron transport in dual layer solid targets

N. M. H. Butler, R. J. Dance, D. A. Maclellan, R. J. Gray, P. McKenna *(SUPA/Dept of Physics, University of Strathclyde, Glasgow, UK)*
D. R. Rusby, G. G. Scott, D. Neely *(CLF, STFC Rutherford Appleton Laboratory, Didcot, UK)*
M. P. Desjarlais *(Sandia National Laboratories, Albuquerque, USA)*
B. Zielbauer, V. Bagnoud *(PHELIX Group, GSI Hemholtzzentrum für Schwerionenforschung GmbH, Darmstadt, Germany)*

The influence of lattice structure and low-temperature electrical resistivity on the transport of fast electrons in solids is numerically investigated using 3D hybrid particle-in-cell (PIC) simulation. Simulations of dual layer targets comprising ordered and disordered carbon allotropes, show the effect of electrical resistivity in layered targets that do not exhibit a change in atomic number across the layer boundary.

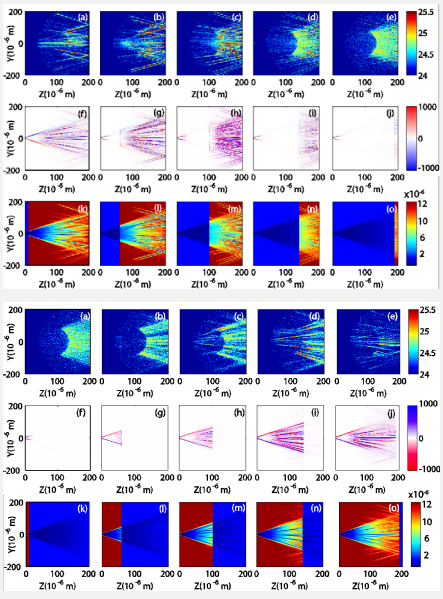

Our numerical investigation implies that there is a minimum propagation distance of approximately 60 μm of vitreous material (and an implied minimum growth-time), required to allow resistive magnetic fields to evolve to the extent that resistive filamentation of the fast electron beam is observed. In addition, the presence of carbon with disordered lattice structure generates strong filamentary effects, with little dependence on its location within a dual layer target, when its thickness is of the order of 60 μm or greater.

Contact: N. M. H. Butler (nicholas.m.butler@strath.ac.uk)

Top: Zephyros simulation results for double layer targets with vitreous carbon as the front layer and diamond as the rear.
TOP ROW: Log_{10} fast electron density maps (m^{-3}), in the [Y-Z] mid-plane, for: (a) LF =10 μm; (b) LF =50 μm; (c) LF =100 μm;
(d) LF =140 μm; (e) LF =190 μm;
MIDDLE ROW: Corresponding 2D maps of the magnetic flux density (B_x component in Tesla);
BOTTOM ROW: Corresponding 2D maps of electrical resistivity (Wm).

Bottom: Zephyros simulation results for double layer targets with diamond as the front layer and vitreous carbon as the rear.
TOP ROW: Log_{10} fast electron density maps (m^{-3}), in the [Y-Z] mid-plane, for: (a) LF =10 μm; (b) LF =50 μm; (c) LF =100 μm;
(d) LF =140 μm; (e) LF =190 μm;
MIDDLE ROW: Corresponding 2D maps of the magnetic flux density (B_x component in Tesla);
BOTTOM ROW: Corresponding 2D maps of electrical resistivity (Wm).